

DESIGN IMPROVEMENT OF THE RIA 80.5 MHZ RFQ

Q. Zhao*, V. Andreev, M. Doleans, D. Gorelov, T. Grimm, W. Hartung, F. Marti, S.O. Schriber, X. Wu, R.C. York, NSCL, Michigan State University, East Lansing, MI 48824, USA

Abstract

An 80.5 MHz, continuous-wave, normal-conducting, radio-frequency quadrupole (RFQ) was designed for the front end of the Rare Isotope Accelerator (RIA) driver linac. It will accelerate various ion beams (hydrogen up to uranium) from 12 keV/u to about 300 keV/u. The 4-meter-long RFQ accepts the pre-bunched beams from the low energy beam transport (LEBT) and captures more than 80% of the beams with a current of ~0.3 mA. Beam dynamics simulations show that the longitudinal output emittance is small for both single- and two-charge-state ion beams with an external multi-harmonic buncher. A 4-vane resonator with magnetic coupling windows was employed in the cavity design to provide large mode separation, high shunt impedance, and a small transverse dimension. The results of beam dynamics as well as the electromagnetic simulations are presented.

INTRODUCTION

To minimize beam losses in the RIA driver linac, the superconducting (SC) linac requires the front end to provide a longitudinal beam emittance of about 1.2π -keV/u-ns (99.5% particles) with minimum transverse emittance growth. Since the beam current is not very high in the RIA driver linac, the dc beam selected from the ion source can be efficiently pre-bunched by an external multi-harmonic buncher before injection into the RFQ. This scheme can produce a smaller longitudinal output emittance [1], and enhance the RFQ's acceleration efficiency. In previous designs of the front end RFQ [2,3], the longitudinal output emittance was larger than the requirement when using a more realistic input beam from LEBT that includes unbunched particles. Therefore, we optimized the initial longitudinal acceptance and its evolution to remove the tails while still maintaining the transverse emittance. Beam dynamics simulations showed about 83% of the injected beam was accelerated with required output emittances. In addition, an improved 4-vane RFQ structure with coupling windows was adopted to achieve improved mode separation and smaller power dissipation.

The driver linac will provide ion beams from protons up to uranium. To meet the final beam power requirement for heavier ions, two charge-state beams will be injected and accelerated in alternate longitudinal buckets of the RFQ [4]. Since the heaviest ion beams are the most challenging, the baseline design has been primarily focused on the uranium beam with charge states of 28+ and 29+. Therefore, the RFQ must be able to operate with a wide range of power levels to accommodate the different ion species. To minimize the range of voltages,

we proposed to use triatomic hydrogen molecule ions (e.g. H_3^+ instead of H^+ for proton) from the ion source through the RFQ and first segment of SC linac until stripped into monatomic ions at first stripper, which also reduces the beam current by a factor of 3 at the low energy side.

DESIGN PHILOSOPHY

The 100% duty factor, normal conducting RFQ will accelerate ion beams from 12 keV/u to about 300 keV/u. The input energy is determined by the high voltage platform of ion source, while the output energy is set to obtain a transit time factor of 0.5 for the first SC cavity in the driver linac and is a tradeoff between the acceptance of the SC linac and the size of RFQ. The 80.5 MHz frequency is chosen to be the same as the successive quarter-wave superconducting structures.

The design goals are the minimization of the longitudinal and transverse emittance, RF power requirements and structure size. For the RIA beam currents, an external harmonic buncher with a quasi-linear bunching field can generate a small longitudinal emittance beam for RFQ. To obtain a low output emittance, the RFQ should only accept the well-bunched core particles for further acceleration avoiding capture of the small fraction particles in the tails of the distribution. Since the beam is already bunched at the entrance of RFQ, an initial synchronous phase of -30° and a modulation factor of 1.03 are chosen so that the longitudinal acceptance is truncated, as shown in Fig. 1. These values represent an optimization between the removal of tail particles and providing a linear field for the bunched particles. The modulation factor as well as the synchronous phase is then smoothly increased to accelerate just the core particles.

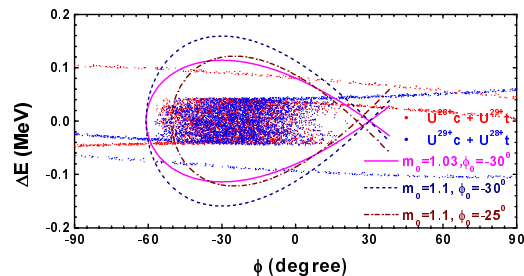


Figure 1: Initially reduced separatrices with bunched beams.

Even though the beam is pre-bunched, a four-cell radial matcher was found to be of benefit especially for a two-charge-state beam. A reduced adiabatic bunching design before the acceleration section is necessary to achieve stable bunches and control the blowup of emittances. Particles with large transverse amplitudes may result in

* zhao@nscl.msu.edu

large longitudinal amplitudes due to the coupling between the two motions. Hence, proper transverse focusing must be provided to maintain a small beam envelope. The transverse phase advance is larger than the longitudinal one to avoid a coupling resonance.

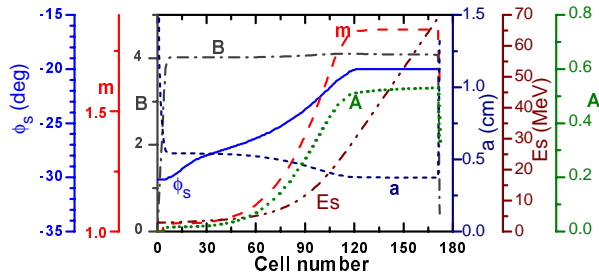


Figure 2: Evolution of the synchronous phase (ϕ_s), modulation factor (m), transverse focusing strength (B), minimum radius aperture (a), synchronous beam energy (E_s), and acceleration efficiency (A) along the RFQ.

Fig. 2 shows the main RFQ parameters as a function of cell number. The focusing strength was held constant ($B=4.1$) along the structure leading to a constant average aperture radius of 5.5 mm, keeping the capacitance independent of longitudinal position to facilitate cavity tuning. In this scheme, the minimum vane radius decreases with the increase of modulation factor along the RFQ and determines the normalized transverse acceptance of about 1.4π -mm-mrad. A nominal inter-vane voltage of 70 kV was adopted in the design resulting in a moderate peak surface electric field of $1.58 \cdot E_{kilpatrick}$. The transverse phase advance per focusing period is around 25° and is almost constant along the RFQ, while the phase motion of the longitudinal oscillation is approximately 15° . The transverse geometry of the vane-tip is circular with the same transverse radius of curvature throughout the RFQ making fabrication easier. The ratio between the vane tip radius and the average radial aperture was chosen to be 0.82 as a compromise between the peak voltage and the effect of multi-poles. A radial matcher at the exit of the RFQ [5] was used to obtain an output beam with similar Twiss parameters in both horizontal and vertical planes to match to the downstream solenoidal focusing.

BEAM DYNAMICS

The beam dynamics simulations of the RFQ were performed with the PARMTEQ code [6]. The baseline design was for $^{238}\text{U}^{28+}$ and $^{238}\text{U}^{29+}$ with charge-to-mass of 0.12. PARMELA output from the LEBT was used as the input beam distribution for PARMTEQ. The phase spaces of the two-charge state beam at the RFQ entrance and exit are plotted in Fig. 3, where $^{238}\text{U}^{28+}$ and $^{238}\text{U}^{29+}$ were plotted in the same spaces, although they were separated by an rf period [4]. The longitudinal input phase space was determined by the harmonic buncher in the LEBT. Fig. 4 illustrates the evolution of the rms beam emittance and transmission along the RFQ for the two-charge-state beam. About 83% of the beam was captured and accelerated by the RFQ. There was no transverse

emittance increase of the two-charge-state beam throughout the RFQ. The rms and 99.5% of longitudinal output emittances are 0.1 and 1.2 π -keV/u-n, respectively, which is slightly larger than that of the single-charge-state beam. This increase is mainly due to the phase-shift between the beams and may be minimized.

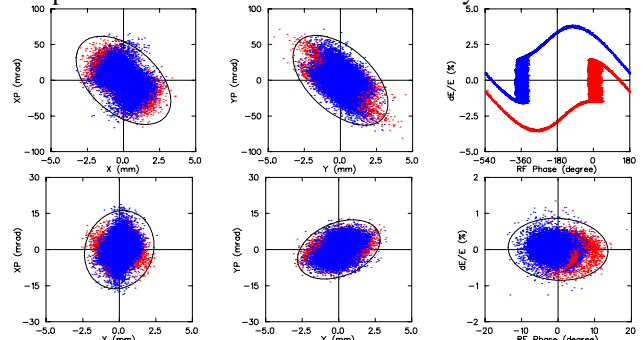


Figure 3: Phase space distributions of two-charge-state uranium beam at the entrance (above) and the exit (below) of RFQ ($^{238}\text{U}^{28+}$ in red, $^{238}\text{U}^{29+}$ in blue).

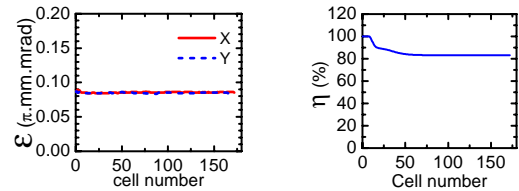


Figure 4: Variations of normalized transverse rms emittance and beam transmission along RFQ for $^{238}\text{U}^{28+}$ and $^{238}\text{U}^{29+}$.

The beam dynamics of other ions are similar after scaling the inter-vane voltage according to the corresponding charge-to-mass ratios. Triatomic hydrogen molecule H_3^+ instead of H^+ will be accelerated in the RFQ to increase the operation voltage. Fig. 5 shows the phase space of a H_3^+ ion beam at the entrance and exit of RFQ, which are analogous to those of two-charge-state beam.

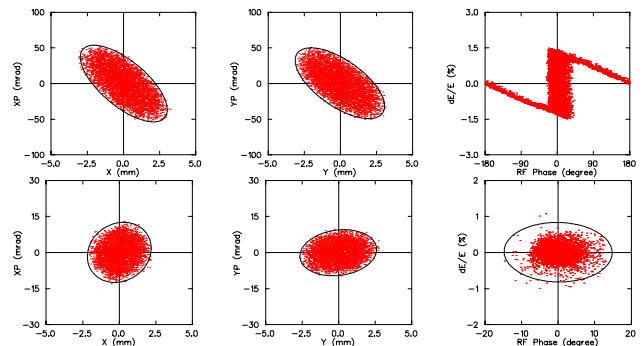


Figure 5: Phase space distributions of H_3^+ beam at the entrance (above) and the exit (below) of RFQ.

RESONANT STRUCTURE

The design of the RFQ cavity is based on the improved 4-vane resonator with magnetic coupling windows [7], as shown in Fig. 6. The windows improve the azimuthal and longitudinal stabilization of the operating mode (a

combination of TE₂₁₁ and coaxial one) by increasing the separation from parasitic modes, and significantly reduce the transverse dimensions of the resonator. Test results of such structures confirmed the high RF efficiency as well as the simplicity of alignment and tuning [8].

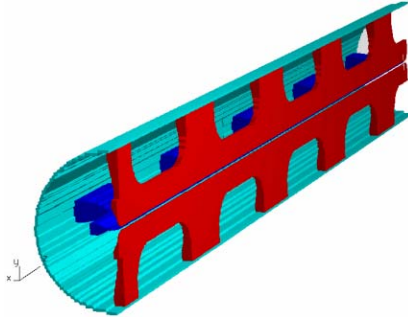


Figure 6: Layout of the 1/2 resonator without end flanges.

The resonator was designed using MAFIA version 4.1. Table 1 lists the main parameters of the structure. Increasing resonant cell length and window area improve mode separation, but also reduces shunt impedance of the resonator. A separation of 13.3 MHz from the nearest dipole mode was obtained, which would be sufficient to avoid problems of alignment and tuning from experience [8]. The shape of the windows has been optimized to reduce the extra magnetic flux density and rf losses. The magnetic field in y-z plane and electric field in x-y plane are shown in Fig. 7, respectively. Sufficient water-cooling is provided to maintain a good thermal stability during cw operation.

Table 1: Main parameters of the RFQ resonator

Name (unit)	Value
Resonator length (m)	4
Tank inner diameter (m)	0.54
Resonant cell number	9
Window width (m)	0.56
Window height (m)	0.17
Average aperture radius (cm)	0.55
Vane tip radius (cm)	0.45
Operating mode frequency (MHz)	80.5
Nearest quadrupole mode (MHz)	88.6
Nearest dipole mode (MHz)	93.8
Specific shunt impedance (kΩ·m)	389
Quality factor	13000
Inter-vane voltage (kV)	70
Peak electric field (MV/m)	14
Peak magnetic field (mT)	11
Total power dissipation (kW)	51

A flat inter-electrode voltage along the vanes has been achieved, as plotted in Fig.8, by properly tuning the end cells of the cavity with a 3-cm undercut on the vanes at both ends of the structure. The ripple of the inter-vane voltage, an inherent feature for all longitudinally non-uniform RFQs, is ±0.35%. In addition, 9 tuners with diameter of 8 cm will be used in each quadrant to provide misalignment compensation and frequency tuning.

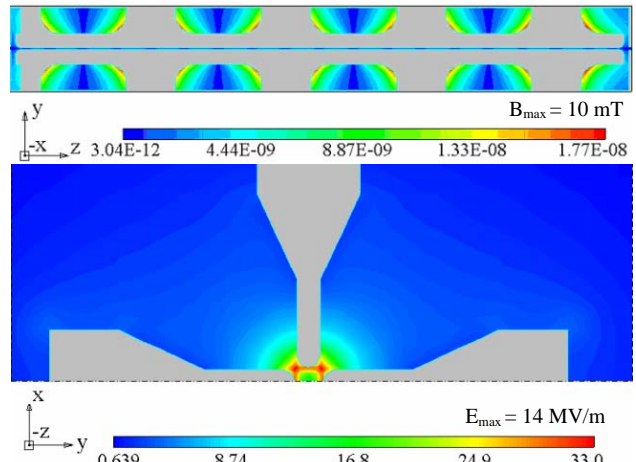


Figure 7: Magnetic flux density in y-z cross section (vertical vanes) on the top, and electric field in x-y cross section (half of the resonator) on the bottom.

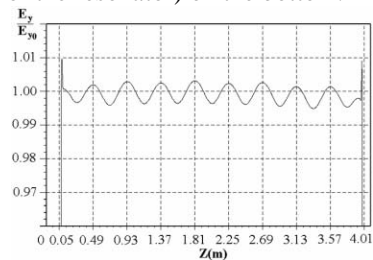


Figure 8: Distribution of the normalized inter-vane voltage.

SUMMARY

Beam dynamics simulations show the RFQ can produce required output emittance for both two and single charge-state beams with the input from the LEBT. The resonator has good mode separation, low power dissipation, and small inter-vane voltage variation.

ACKNOWLEDGEMENTS

We are grateful to Drs. T. Wangler at LANL, H. Podlech at IAP and R. Duperrier at CEA for the helpful discussions, and wish to thank Drs. L. Young, J. Billen and R. Garnett at LANL to provide the simulation codes. This work has been supported by Michigan State.

REFERENCES

- [1] J.W. Staples, Proc. Linac'94, Tsukuba, Japan, p755.
- [2] H. Podlech, et al., Proc. EPAC'02, Paris, France, p.945.
- [3] R. Duperrier, NSCL internal report, 2002
- [4] P.N. Ostroumov, et al., Proc. Linac'00, Monterey, USA, p202.
- [5] K. Crandall, Proc. Linac'94, Tsukuba, Japan, p.227.
- [6] K. Crandall, et al., LANL Report 96-1836, 2004.
- [7] V.A. Andreev and G. Parisi, Proc. PAC'93, Washington DC, USA, p3124; V.A. Andreev and G Parisi, Proc. EPAC'94, London, UK, p1300.
- [8] V.A. Andreev, et al., Proc. PAC'97, Vancouver, Canada, p1090; G. Bisoffi, et al., Proc. EPAC'00, Vienna, Austria, p324.